

Iron Deficiency Anemia Detection using Machine Learning Models: A Comparative Study of Fingernails, Palm and Conjunctiva of the Eye Images.

Justice Williams Asare¹, PETER APPIAHENE¹, Emmanuel Timmy Donkoh¹, and Giovanni Dimauro²

¹University of Energy and Natural Resources

²Università degli Studi di Bari Aldo Moro

February 6, 2023

Abstract

Anemia is one of the global public health challenges that particularly affect children and pregnant women. A study by WHO indicates that 42% of children below 6 years and 40% of pregnant women worldwide are anemic. This affects the world's total population by 33%, due to the cause of iron deficiency. The non-invasive technique, such as the use of machine learning algorithms, is one of the methods used in the diagnosing or detection of clinical diseases, which anemia detection cannot be overlooked in recent days. In this study, machine learning algorithms were used to detect iron-deficiency anemia with the application of Naïve Bayes, CNN, SVM, k-NN, and Decision Tree. This enabled us to compare the conjunctiva of the eyes, the palpable palm, and the colour of the fingernail images to justify which of them has a higher accuracy for detecting anemia in children. The technique utilized in this study was categorized into three different stages: collecting of datasets (conjunctiva of the eyes, fingernails and the palpable palm images), preprocessing the images; image extraction, segmentation of the Region of Interest of the images, obtained each component of the CIE L*a*b* colour space (CIELAB). The models were then developed for the detection of anemia using various algorithms. The CNN had an accuracy of 99.12% in the detection of anemia, followed by the Naïve Bayes with an accuracy of 98.96%, while Decision Tree and k-NN had 98.29% and 98.92% accuracy respectively. However, the SVM had the least accuracy of 95.4% on the palpable palm. The performance of the models justifies that the non-invasive approach is an effective mechanism for anemia detection. Keywords: Iron deficiency, anemia, non-invasive, machine learning, data augmentation, algorithms, region of interest.

Iron Deficiency Anemia Detection using Machine Learning Models: A Comparative Study of Fingernails, Palm and Conjunctiva of the Eye Images.

Justice Williams Asare^{1*}, Peter Appiahene^{1*}, Emmanuel Timmy Donkoh², Giovanni Dimauro³

1. Department of Computer Science and Informatics, University of Energy and Natural Resources, Sunyani, Ghana

2. Department of Basic and Applied Biology, University of Energy and Natural Resources, Sunyani, Ghana

3. Università degli Studi di Bari 'Aldo Moro', Italy. Coordinatore del Consiglio di Interclasse dei Corsi di Studio in Informatica. Dipartimento di Informatica

*Corresponding Authors: Justice Williams Asare (justice.asare.stu@uenr.edu.gh)

Peter Appiahene (peter.appiahene@uenr.edu.gh)

Abstract

Anemia is one of the global public health challenges that particularly affect children and pregnant women. A study by WHO indicates that 42% of children below 6 years and 40% of pregnant women worldwide are anemic. This affects the world's total population by 33%, due to the cause of iron deficiency. The non-invasive technique, such as the use of machine learning algorithms, is one of the methods used in the diagnosing or detection of clinical diseases, which anemia detection cannot be overlooked in recent days.

In this study, machine learning algorithms were used to detect iron-deficiency anemia with the application of Naïve Bayes, CNN, SVM, k-NN, and Decision Tree. This enabled us to compare the conjunctiva of the eyes, the palpable palm, and the colour of the fingernail images to justify which of them has a higher accuracy for detecting anemia in children.

The technique utilized in this study was categorized into three different stages: collecting of datasets (conjunctiva of the eyes, fingernails and the palpable palm images), preprocessing the images; image extraction, segmentation of the Region of Interest of the images, obtained each component of the CIE L*a*b* colour space (CIELAB). The models were then developed for the detection of anemia using various algorithms.

The CNN had an accuracy of 99.12% in the detection of anemia, followed by the Naïve Bayes with an accuracy of 98.96%, while Decision Tree and k-NN had 98.29% and 98.92% accuracy respectively. However, the SVM had the least accuracy of 95.4% on the palpable palm.

The performance of the models justifies that the non-invasive approach is an effective mechanism for anemia detection.

Keywords: Iron deficiency, anemia, non-invasive, machine learning, data augmentation, algorithms, region of interest.

1. Introduction

Anemia is a serious public health problem that mostly affects children and pregnant females globally. A study by the WHO indicates that 42% of children below the age of 6 and 40% of females who are pregnant worldwide are anemic [1], [2]. Anemia affects the world's population of 33% due to iron deficiency [3]. Anemia occurs once the level of red blood cells within the body decreases or when the structure of the red blood cells is destroyed or weakened [4].

Throughout the pregnancy period, the plasma level is reduced to 50%, while the mass ranges from 18% – 20% in Hb and red blood cells to 33% [5]. A procedure that is complex and comprehensive takes place in the human body for the regeneration of red blood cells after the loss of blood. Anemia can also occur when the Hb level in the red blood cell is below the normal threshold, which results from one or more increased red cell destruction, blood loss, defective cell production or a depleted sum of Red Blood Cells [6]. Early detection symptoms of anemia are an ideal primary stage to alleviate it because if the detection and treatment of anemia are delayed, it irreversibly damage the human organ, which can lead to death in some instances [7].

Hb carries oxygen from the lungs to tissues, and carbon dioxide is returned from the tissue of the lungs, which is considered to be an essential task in the human body. This also performs an estimation of the Hb level for analysis of blood to detect either one is anemic or not. The level of Hb usually determines whether one is anemic or not [8].

Iron deficiency anemia has additionally been shown to affect psychological features and physical development in children and cut back productivity in adults [9]. Long-term illness can also contribute to a patient's risk of diagnosing anemia. Syndromes that mingled with the sophisticated prevalence of anemia include diabetes, kidney syndrome, cancer, human immunodeficiency virus, that is, (HIV/AIDS), inflammatory bowel disease (IBD), and cardiovascular disease [10]. Malaria, bilharzia, and hemoglobinopathies are other main contributors [1], [10].

The clinical approaches used are based on the extraction of blood, which requires higher labour and costs of instrumentation, and is a time-ingesting technique that exposes health workers to blood-transmissible diseases [11]. In numerous health centres, evaluation of eye conjunctiva pallor is usually used to detect anemia that turns out to be rapid. Medical officers usually pull down the protective fold (the lid of the eye) and subjectively assess or examine the colour of the conjunctiva of the eye [8], [12].

In several cases, the clinical sign for the detection of anemia will move and be quite helpful, but the lack of agreement between observers on several things and the low sensitivity of the conjunctiva colour will undermine the authenticity of the visual detection method [13], [14]. This examination is not precise and is not reliable since the quality of these findings depends on the decision and training of the health officer [15].

Numerous emerging geographical areas are vulnerable to anemia due to inadequate health and medical facilities with few health workers, such as medical officers and laboratory technicians or biomedical scientists. The potential risk of anemia can be diagnosed and monitored by using the non-invasive method and smartphone-based devices which is cost-effective, takes less time, and more promising in focusing on these health issues [15]. This state of affairs may be lessened without the involvement of blood assessment that is costive and inaccessible in several areas which makes the detection of anemia complex in its early stage [11].

This study aims to detect anemia using a non-invasive method, which is a comparative study of machine learning algorithms (Naïve Bayes, CNN, SVM, k-NN, and Decision Tree) with the use of images of the palpable palm, the colour of the fingernails and conjunctiva of the eyes.

2. Related Works

In recent times, the use of computerized algorithms such as Machine Learning for the estimation of Hb and the diagnosing or detection of medical diseases such as anemia is commonly related with high accuracy to analyzing the colour of nailbeds, conjunctiva of the eyes and the palpable palm from digital photographs taken by smartphones [16]. By classifying the basic set of algorithms, the quintessence of the classification method types such as the Support Vector Machine, K-Nearest Neighbor, Bayesian Networks, Artificial Neural Networks, and Decision Tree classifier is considered, showing comprehensive data mining algorithms and a group of their essentiality type.

[17] indicated that specifically the best algorithms for classification or detection are based on the domain of the problem to be solved. However, there are limited attributes used for only a few blood parameters [18]. The study conducted by [19] used a non-invasive technique to detect anemia with the help of clinical symptoms based on the fingernails and palm with their intensity colour. They extracted the RGB component of 20 images and utilized the Naïve Bayes algorithm which achieved an accuracy of 90%. [20] used different attributes that included age, sex, symptoms, chronic diseases, and blood parameters in consultation with experienced medical consultants. The study utilized notable methods such as ANN, SVM, and decision tree-based methods and Naïve Bayes, K-NN and rule-based approaches were applied to the Hb value.

For detecting anemia using a non-invasive method, a lot of research has been conducted using conjunctiva images of the eye. [7], [21] used a Support Vector Machine (SVM) to computerise a non-invasive model to detect anemia using 19 conjunctivae in the eye images. The images corresponded to their various hemoglobin levels known, which attained an accuracy of 78.90% in 15 out of the 19 cases. [21] used the least squares support vector machine (LS-SVM) to detect anemia using conjunctiva images of the eyes using the application of image processing and computer vision. The procedure resulted in a precision of 85%, a sensitivity of 92%, and a specificity of 70%. The study used 77 tested images, of which 21 were non-anemic while 56 were anemic.

Similarly, [22] compared the results of their study with those of the laboratory test that yielded a sensitivity and specificity of 91.89% and 85.18%, respectively, when images of the conjunctiva and tongue were used with the application of Logistic Regression and neural network Algorithms,

while, [23] applied the neural network of convolution with the aid of segmented images of the conjunctiva to detect anemia, which obtained a sensitivity of 77.58%. The results were compared with laboratory tests. Furthermore, [9] detected anemia using the image of the conjunctiva of the eyes. A new device for image capture was proposed based on the use of the k-Nearest Neighbor (k-NN) algorithm, which achieved 90.26% accuracy using nonanemic images of 84 patients and anemic images of 29 patients. [6] stated that the use of the conjunctiva alone to detect anemia in children is not enough, as exposing the conjunctiva could expose them to germs, bacteria, or falling objects; hence, the use of the palpable palm was recommended.

From the reviewed related works, it is evident that non-invasive techniques such as machine learning algorithms are efficient, cost-effective and provide timely results in medical diseases diagnosing such as anemia detection. Furthermore, since most studies used the conjunctiva of the eyes, this study compared the performance of the conjunctiva of the eyes, palpable palm and colour of the fingernails in the detection of anemia. This is because exposure of the conjunctiva of children may be exposed to infections or falling objects and the palm is also one of the important points of the human body for the detection of anemia [6], [24], hence the need to compare its performance (conjunctiva of the eyes, palpable palm, and colour of the fingernails) performance in the detection of anemia.

3. Methodology and Experimental Design

This section deals with the procedure and algorithms used for the proposed models. The method proposed for this study was made up of three stages;

Stage I – Image Capturing (dataset collection); taking images of the palpable palms, conjunctivae of the eyes, and fingernails.

Stage II – Preprocessing of Images; extraction of the Region of Interest of the captured images. Afterwards, we separated the component of the CIE $L^*a^*b^*$ (also known as CIELAB) colour space of the images, segmented the images, and calculated the mean intensity of the various CIE $L^*a^*b^*$ colour space components of the images (extraction and segmentation of the ROI).

Stage III – Development of the detective (anemic or non-anemic) models. Machine learning algorithms (Naïve Bayes, CNN, SVM, k-NN, and Decision Tree algorithms) were developed to detect anemia using various captured and processed images (datasets).

This means that for anemia to be detected, the dataset goes through three phases or steps.

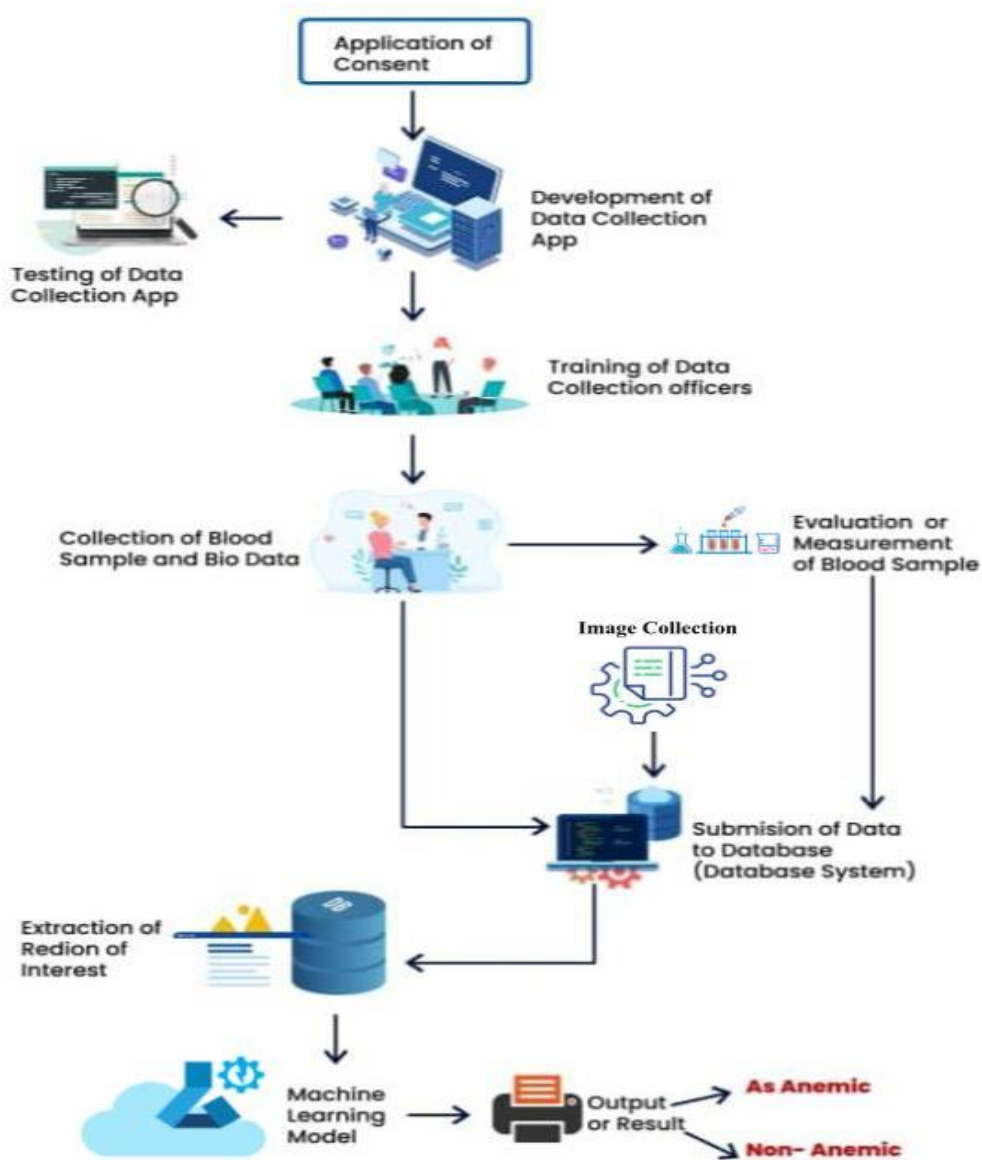


Figure 1: A conceptual framework for the proposed methodology

3.1 Data Collection System and Datasets

The system used for data collection was developed using Kobo Collect (v2021.2.4) installed on mobile tablets (Samsung Galaxy Tab 7A). The biodata of the patients/participants such as Hb values, age, sex, and remark (anemic or non-anemic) based on the Hb value captured with the corresponding images (conjunctiva of the eyes, palpable palm and fingernails) and uploaded to the cloud storage (database). This was carried out by professional (licenced) biomedical scientists who underwent a week-long proficiency training at the Centre for Research in Applied Biology, University of Energy and Natural Resources, Sunyani, Ghana, on how to capture images of children aged 6 to 59 months. The Committee for Human Research and Ethics reviewed and approved (Reference number: CHRE/CA/042/22) this study before its commencement.

Regarding the conjunctiva of the eyes, the lower eyelid was pulled slightly with the thumb and index finger to take the image. On the palm, due to the reason that the participants were children, the biomedical scientists held the hand of the participant and stretched the palm through the fingers and then captured images of the palm. On the fingernails, the wrist hand of the participant was held by the biomedical scientists and a photograph of the fingernails was captured.

However, to avoid disproportionate gleam effects on the image quality that might affect the models' performance, the flashlights of the cameras were off when taking the photographs of the images. This mechanism served as a great measure to eradicate the influence of ambient light in the images.

After the images (datasets) were received through the cloud storage (database), they were extracted using the triangle thresholding algorithm and the images were augmented to increase the data size. Afterwards, the images were segmented into their various CIE L*a*b* colour spaces. The datasets were collected from 10 health facilities across the country (Appendix A: List of hospitals). These included districts (n=7), regional (n=2), and tertiary (n=1) hospitals. This study's dataset focuses on children aged 5 to 59 months. The datasets used Hb value; <11 g/dL is anemic, while, >=11 g/dL is non-anemic.



Figure 2: Image description of how the dataset photographs were taken

Table 1: Samples of biodata (dataset) collected from selected participants for the study

Image_ID	Hb_Level	Age	Gender	Remarks
Image_001	8.9	2	Male	Anemic
Image_002	12	5	Male	Non-anemic
Image_003	12	4	Female	Non-anemic
Image_004	12	4	Male	Non-anemic
Image_005	9.9	5	Male	Anemic
Image_006	12	1	Female	Non-anemic
Image_007	12	1	Male	Non-anemic
Image_008	12.5	3	Female	Non-anemic
Image_009	9.9	4	Male	Anemic
Image_010	12	2	Female	Non-anemic
Image_011	8.9	4	Male	Anemic
Image_012	9.9	3	Female	Anemic
Image_013	8.9	2	Female	Anemic
Image_014	8.95	2	Male	Anemic
Image_015	12	2	Female	Non-anemic
Image_016	12.5	5	Male	Non-anemic



A



B

Figure 3: Raw images of the conjunctiva of the eyes, palpable palm, and colour of the fingernails, where [A] is for non-anemic images and [B] is for anemic images.

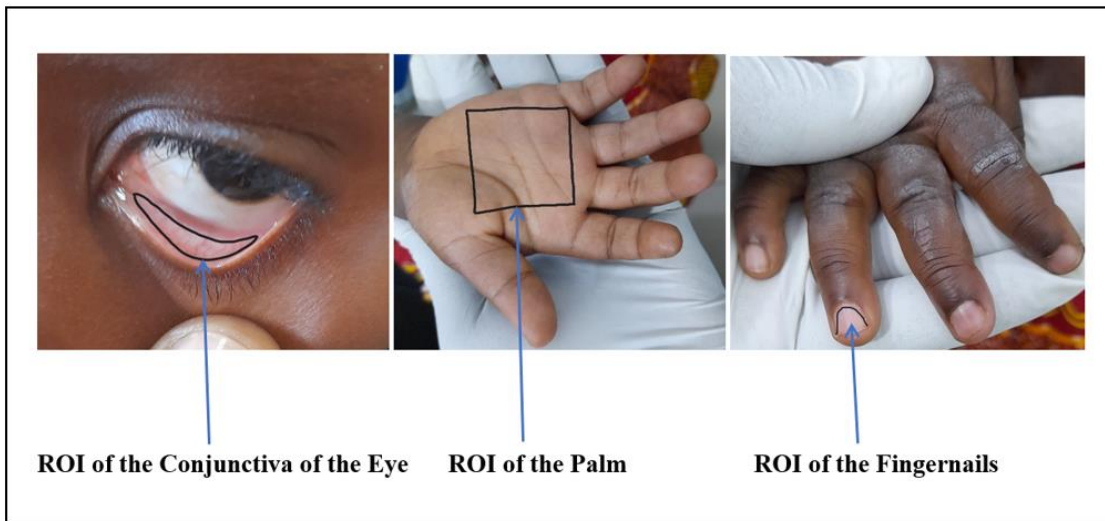


Figure 4: Region of interest (ROI) of Image

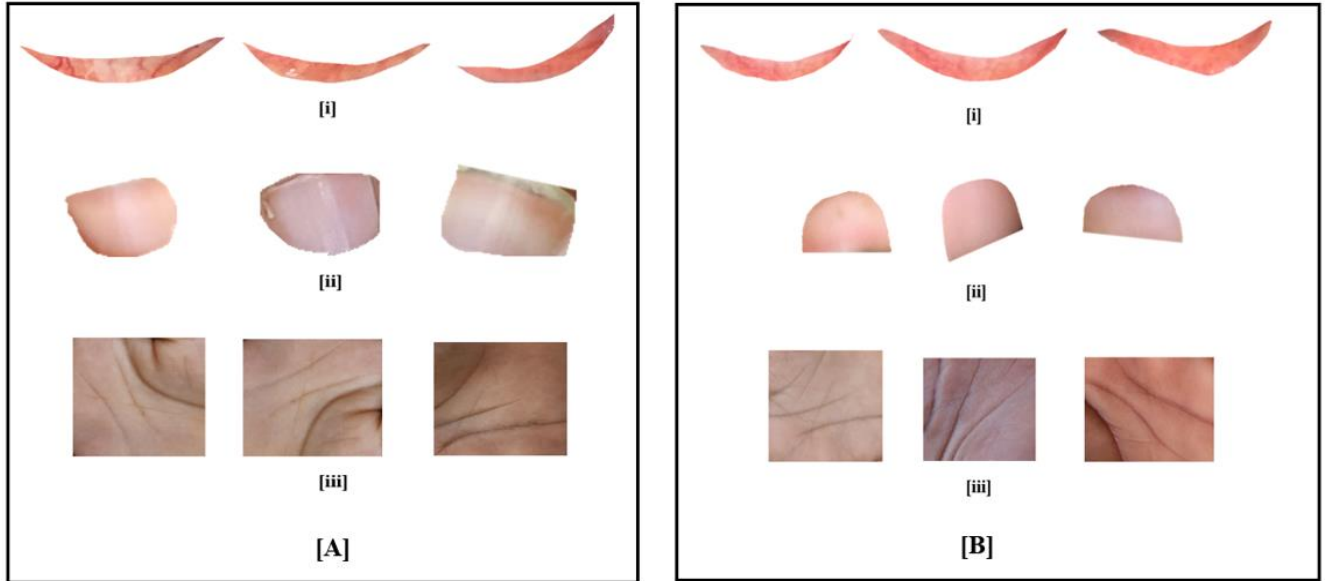


Figure 5: Sample of Extracted images where [A] are anemic images and [B] are non-anemic images. [i], [ii], and [iii] are conjunctiva of the eyes, the colour of the fingernails, and the palpable palm respectively, for both [A] and [B] (anemic and non-anemic) images.

Table 2: Original image dataset for the detection of anemia

Original Image Dataset	Anemic	Non-anemic	Total Dataset
Conjunctiva of the eyes	304	223	527
Palpable palms	304	223	527
Colour of the fingernails	304	223	527
Total	912	669	1581

Table 3: Dataset after Image Augmentation for the detection of anemia

Dataset after Image Augmentation	Anemic	Non-anemic	Total Dataset
Conjunctiva of the eyes	1520	1115	2635
Palpable palms	1520	1115	2635
Colour of the fingernails	1520	1115	2635
Total	4560	3345	7905

3.2 Image Augmentation

For higher accuracy to be derived, machine learning models need to be trained on a large dataset. The small size of the dataset is capable of resulting in overfitting [25]. This is due to the reason that during the training and testing stage, data samples that are small in number are not able to be generalised and used for hyperparameter models.

Image augmentation techniques are used to execute procedurals on images that are artificially generated such as rotation, shift, flip, translation, etc. Anemia dataset is hard to come by, as a result, this study uses image argumentation to expand the dataset sample for training, testing and validation of the model.

- **Rotation:** in the rotation of the image augmentation, the actual image is rotated 90° and 270° to acquire the artificial image with the values of the mean intensity of the image remaining the same as the positioning of the images varies. The mathematical model for rotation image augmentation;

The rotation angle θ for the equations for the new coordinates of a pixel is defined as:

$$x' = x \cos \theta - y \sin \theta \dots \dots \dots \text{eqn. (1)}$$

$$y' = x \sin \theta + y \cos \theta \dots \dots \dots \text{eqn. (2)}$$

in an anti-clockwise rotation. In an analogous formulation, the position of every pixel (x' , y') in the new image can be written as a vector and the rotation matrix:

$$\begin{bmatrix} x' \\ y' \end{bmatrix} = \begin{bmatrix} \cos \theta & -\sin \theta \\ \sin \theta & \cos \theta \end{bmatrix} \begin{bmatrix} x \\ y \end{bmatrix} \dots \dots \dots \text{eqn. (3)}$$

The rotation (x_0, y_0) is the coordinates (0, 0) point of derivation which rotates at the mid-point of the image or around a certain point. For an image or a pixel to rotate around a point (x_0, y_0) subjectively the equation is expressed as;

$$x' = x_0 + (x - x_0) \cos \theta + (y - y_0) \sin \theta \dots \dots \dots \text{eqn. (4)}$$

$$y' = y_0 + (x - x_0) \sin \theta + (y - y_0) \cos \theta \dots \dots \dots \text{eqn. (5)}$$

The pixel at the position (x_0, y_0) is the only pixel that does not move from its position. If an additional image is intended from the original image one, x and y then describe the equation which needs to be solved.

- **Flipping:** For the enhancement of different forms of artificial images, the original images can be vertically or horizontally flipped as the positioning of this operation is altered, while the features and components of the values of the mean intensity remain unchanged.

The inverse of the coordinates places the new image outside the old image, and where there is the ought for the image to be flipped or mirrored along the y-axis, the new image presented requires to be translated also by the image height, with the mathematical models stated below;

$$x' = x \dots \dots \dots \text{eqn. (6)}$$

$$y' = y_{max} - y \dots \dots \dots \text{eqn. (7)}$$

The operations only operate integers of the coordinates and the margins of the image which are new to be ordinarily equal to the old image margins without any interruption.

- **Translation:** the ROI of the actual images are marginally shifted to either the X and Y directions or mutually. The translation operation does not change the values of the image component of the mean intensity.

The mathematical models for translation in the image augmentation are enlisted in the equations below;

$$x' = x + xT \dots \dots \dots \text{eqn. (8)}$$

$$y' = y + yT \dots \dots \dots \text{eqn. (9)}$$

Where the original coordinates of x and y are the coordinates of x' and y' in the new image denoted by the coordinates of a pixel P , as P is translated by a distance in every direction expressed as xT and yT correspondingly.

In the process of augmenting the images, the original datasets for each image, (the conjunctiva of the eyes, palpable palm and the fingernails) were rotated 90° , and 270° , flipped (mirrored/mirroring) which was done using the vertical and horizontal method and utilized a translation to the X and Y axis.

Some operations in image augmentation such as Gaussian and cropping are not suitable since they significantly adjust the value of the mean intensity of the image components [25]. After the augmentation of the images was completed, the final datasets in Table 3 were used.

Afterwards, a random selection technique was used to divide the dataset for training which consists of 70% of the total dataset used for training, 10% for validation and 20% for Testing. The size of the dataset for the conjunctiva of the eye, palm and fingernails were of the same (size). All three images were from the same patient/person, and when one of the images (either the conjunctiva, palm, or fingernails) was rejected, all the remaining images from the patient/person were also rejected.

3.3 Machine Learning Models Utilized for the Study

3.3.1 Decision Trees

The decision tree algorithm is effective for the analysis of several variables even though they are simple. Splitting data into branch-like segments is identified by various mechanisms depending on the algorithm used to operate.

3.3.2 Naïve Bayes

With the use of probability based on a given set of features, the Naïve Bayes classifier allows one to predict a class or category and is termed a probabilistic classifier because it incorporates strong independence assumptions based on models of probability.

3.3.3 K-Nearest Neighbor (K-NN) Algorithm

The K-NN algorithm is a supervised ML algorithm which is simple and capable of being used to handle both problems of regression and classification. Even though it has a major drawback of significantly as the data size to be used grows it slows down, and it is easy to be implemented and to be understood.

3.3.4 Support Vector Machines (SVMs)

Support vector machines (SVMs) are a relatively new and widely used family of classification tools that combine several elements of previously used methods. SVMs, like discriminant analysis, start with the assumption that the data are "separable," that is, that they can be split into groups by a functional separator [26]

3.3.5 Convolutional Neural Network

In CNN, the features of images are identified by filters more than once to permit the categorization of objects. There is a kernel edge in the CNN that uses differential values of large pixels to highlight pixels, as these features are extracted with the CNN scheme responsible for the kernel [27].

3.4 Anemia Detection Condition

After pre-processing of images to generate the dataset, the extracted ROI were transformed in the CIELAB (also known as CIE $L^*a^*b^*$) colour space model for each image. The L^*a^*b colour space is envisioned to mimic human vision or perception. It is expressed by the standard deviation value of the ROI a^* elements, which is the mean value. The red components ($a^* > 0$) and green components ($a^* < 0$) are instances of a^* components.

Preceding work in this field illustrates that there exists a resilient affiliation between a^* components and Hb levels when calculated using Pearson Correlation Index, and various experiments were done in this area show that patients with higher values of Hb verge to have an average value of a^* greater than 160 and patients with lower Hb values tend to have an average value of a^* less than one hundred and forty-two [28]. As a result, the average values of a^*

components seem to be more discerning (i.e., the mean intensity of red and green components better differentiates anemic and non-anemic individuals).

To activate the colour characterization, the images were operated using the CIE $L^*a^*b^*$ colour space. This colour space maps all visible to the human eye hues into a three-dimensional integer space enabling device-independent digital representation. The goal of these characterizations is to accurately measure human vision, that is, the images' non-linear approach: standardized changes with time because the aforementioned components correspond to systematic changes in the purported colour.

The relative perceptual differences between two colours in L^* , a^* , b^* may be calculated and approximated by treating each colour as a point in a three-dimensional space (with three components: L^* , a^* , b^*) and taking the Euclidean distance between them. The three coordinates L^* , a^* , and b^* are prevalently constant to a predetermined distance. L^* (Lightness) represents the darkest black at 0 and the brightest white at 100, whereas a^* and b^* are colour channels. The actuality in the Cartesian coordinate system (a^* , b^*) characterizes nonalignment grey. The colours of the foe are displayed on the a^* axis, with red at $a^* > 0$ and green at $a^* < 0$, while the colours of the opponent are depicted on the b^* axis, with yellow at $b^* > 0$ and blue at $b^* < 0$. To determine the confidence redness of the images, the positive a^* values are good indications [29].

Every RGB triplet is translated to a discrete numerical value that reflects the red intensity of the colour as viewed using the perception of human vision to examine the link between the acquired image and the Hb readings of a patient. The initial image is converted to RGB→CIE $L^*a^*b^*$ colour scale (RGB colour component mapped to CIE $L^*a^*b^*$ colour space).

After several experiments, the best detection result was obtained by combining three component features in total, namely a^* , b^* , and the G value retrieved from the RGB component pictures. The L and the values of the RGB components were utilised to filter the input data. The mean values of the attributes a^* , b^* , and G were determined precisely by taking into account just the picture pixels with $\min L < L < \max L$ and $\min R = G = B < \max$. This filtering ensures that picture pixels that are excessively dark or bright are removed, and so the approach given here considers only pixels that allow an accurate pallor assessment of the images.

The equations below are the mathematical models for the CIE L*a*b* colour space demonstration.

$$L^* = 116f\left(\frac{Y}{Y_n}\right) - 16, \dots \dots \dots \text{eqn. (10)}$$

$$a^* = 500 \left\{ f\left(\frac{X}{X_n}\right) - f\left(\frac{Y}{Y_n}\right) \right\}, \dots \dots \dots \text{eqn. (11)}$$

$$b^* = 200 \left\{ f\left(\frac{X}{X_n}\right) - f\left(\frac{Z}{Z_n}\right) \right\}, \dots \dots \dots \text{eqn. (12)}$$

Where $f(s) = s^{\frac{1}{3}}$, for $s > 0.008856$

And $f(s) = 7.787s + \frac{16}{116}$, for $s \leq 0.008856$

The colour difference ΔE between two colours in the CIE L*a*b* (CIELAB) colour space is;

$$\Delta E = \sqrt{(L_2^* - L_1^*)^2 + (a_2^* - a_1^*)^2 + (b_2^* - b_1^*)^2} \dots \dots \dots \text{eqn. (13)}$$

Where the ΔE unity value denotes a Just Noticeable Difference (JND)

3.5 Experimental Setup

In this study, five machine learning algorithms (Naïve Bayes, k-NN, SVM, CNN, and Decision Tree) were used to detect anemia using images of the conjunctiva of the eye, palpable palm and colour of the fingernails. The datasets used were obtained from 527 participants. The images were augmented to 2635 for each (conjunctiva of the eye, palpable palm and colour of the fingernails).

The dataset was randomly divided into 70%, 10% and 20%, and was utilized to train, validated, and tested the models respectively. We employed a 10-fold cross-validation for validating the models. Cross-validation is a modest and effective approach used for classification/detection techniques to evaluate performance. The CNN was trained with the SGD optimization and ReLu as the activation function with a regularization of $\alpha = 0.0001$, with an iteration maximal of 10. The prime function of the activation function is for converting the signal input of the nodes into a

signal output. The CNN would become a linear regression with the absence of the activation function, which would not be proficient in learning models which are complex.

For SVM, Sigmoid was used for the operation with 100 iterations as the limit, cost (c) = 100 and epsilon of regression (ϵ) was assigned to 1.10 while the numerical tolerance was set to 0.1000. The k-NN had 100 number of neighbors as the metric was set to Euclidean with uniform weight. For the Decision Tree, we induced the binary tree minimal number of instances in the leave to 10, while smaller subsets less than 5 were not split and 100 minimal of the trees as the limit.

The experiment was carried out using the Orange Data Mining tool (Version 3.32) on Windows 11 (Enterprise Version) Microsoft Cooperation computer system, 64-bit OS, Intel Core i3 2.4GHz and 2.5GHz processor (8th Generation), 128 solid-state drive (SSD) and a 4GB RAM. Orange is a robust data mining and machine learning toolkit through the use of visual and python programming devised in the late 1990s by the University of Ljubljana at the Bioinformatics Laboratory, Department of Computer and Information Science.

[30] used machine learning algorithms such as Naïve Bayes, k-NN and Decision Tree to detect liver disorder of which the orange data mining software gave a significant result. Similarly, [20] used orange data mining software to diagnose and detect diabetes with the use of Random Forest, ANN, k-NN, SVM, and Decision Tree Algorithms. The ANN achieved the highest accuracy of 90.27%, whereas the least accuracy among the other algorithms was SVM with 64.66% accuracy. This justifies that orange data mining software is efficient and effective for the detection of diseases such as anemia, diabetes and liver disorder.

3.7 Performance Measures

For the performance of the models to be evaluated, AUC, F1 – Score, Precision and Recall were used with a 10-fold validation in the anemia detection models.

$$\text{Accuracy} = \frac{TP+TN}{TP+TN+FP+FN} \dots \dots \dots \text{eqn. (14)}$$

$$\text{Recall} = \frac{TP}{TP+FN} \dots \dots \dots \text{eqn. (15)}$$

$$\text{Specificity} = \frac{TN}{TN+FP} \dots \dots \dots \text{eqn. (16)}$$

$$\text{Precision} = \frac{TP}{TP+FP} \dots \dots \dots \text{eqn. (17)}$$

$$\text{AUC} = \frac{TPR-TNR}{2} \dots \dots \dots \text{eqn. (18)}$$

$$\text{F1-Score} = \frac{2(P.R)}{P+R} \dots \dots \dots \text{eqn. (19)}$$

Where; TP is the True Positive number of samples when predicted and the real values are positive
 TN is the True Negative, FN is the False Negative, P is the Precision, R is the Recall and TNR is
 the True Negative Rate.

4. Results

After the models were trained, validated, and tested on the datasets, the proposed models obtained a significant result. The Convolutional Neural Network (CNN) obtained an accuracy of 98.45% on the conjunctiva of the eyes, 98.33% on the colour of the fingernails, and 99.12 on the palpable palm. The SVM had the lowest accuracy of 89.45% for the conjunctiva of the eyes, 92.96% for the colour of the fingernails and 95.34% for the palpable palm. Table 4 – 6 gives details of the results obtained when the models were tested.

Table 4: Performance of the proposed models in detecting anemia using conjunctiva of the eyes

S/N	Algorithm	Conjunctiva of the Eyes (%)				
		Accuracy	F1-Score	AUC	Precision	Recall
1	CNN	98.45	97.63	99.93	97.64	97.63
2	Naïve Bayes	94.94	92.24	97.74	92.64	91.84
3	Decision Tree	97.32	96.02	97.70	93.67	98.49
4	k-NN	97.96	96.86	99.86	97.60	96.13
5	SVM	89.45	84.53	92.16	81.34	87.98

Table 5: Performance of the proposed models in detecting anemia using fingernails

S/N	Algorithm	Colour of the Fingernails (%)				
		Accuracy	F1-Score	AUC	Precision	Recall
1	CNN	98.33	97.54	99.93	97.64	97.44
2	Naïve Bayes	94.94	92.35	98.01	91.96	92.75
3	Decision Tree	97.18	95.61	97.59	98.41	92.96
4	k-NN	97.89	96.82	99.83	96.21	97.44
5	SVM	92.69	88.62	97.08	91.01	86.35

Table 6: Performance of the proposed models in the detection of anemia using a palpable palm

S/N	Algorithm	Palpable Palm (%)				
		Accuracy	F1-Score	AUC	Precision	Recall
1	CNN	99.12	99.89	99.95	99.79	99.98
2	Naïve Bayes	98.96	99.97	99.98	99.97	99.93
3	Decision Tree	98.29	98.97	99.38	98.77	99.18
4	k-NN	98.92	99.89	99.98	99.79	99.92
5	SVM	95.34	94.59	98.97	95.99	93.23

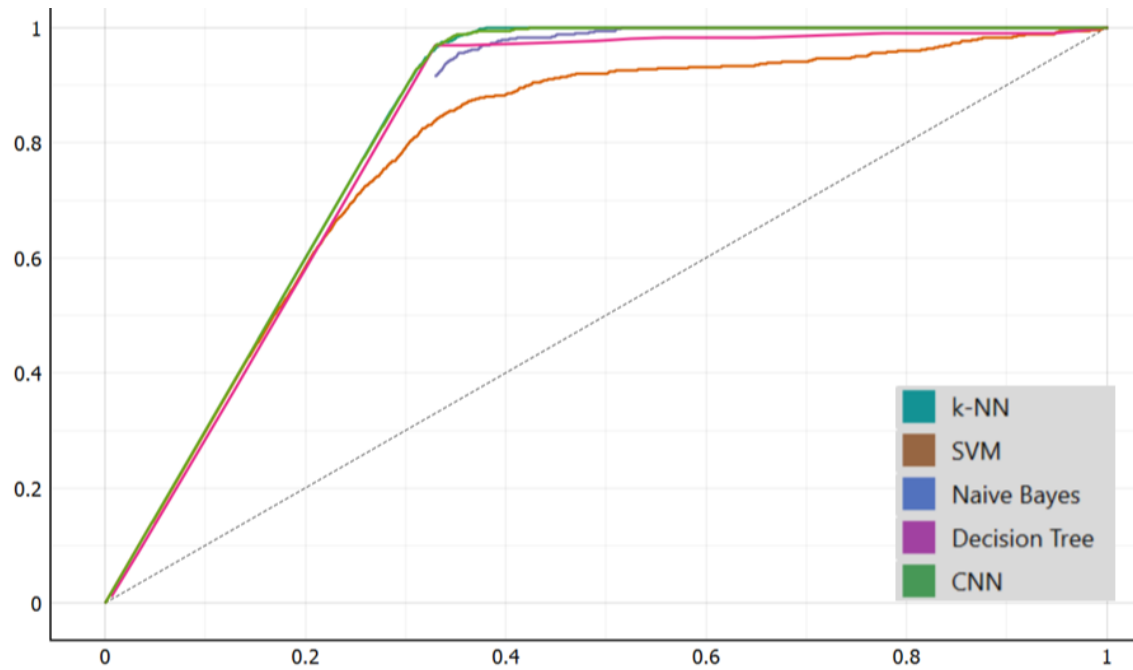


Figure 6: AUC curve of the conjunctiva of the eyes for anemia detection

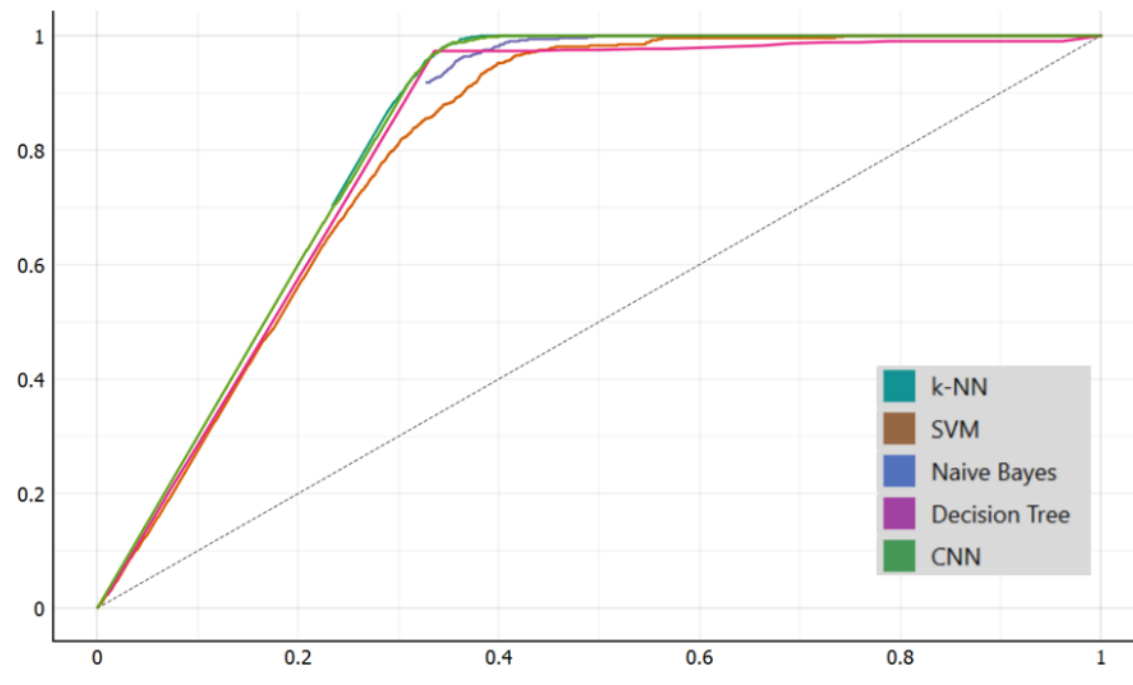


Figure 7: AUC curve of the fingernails in anemia detection

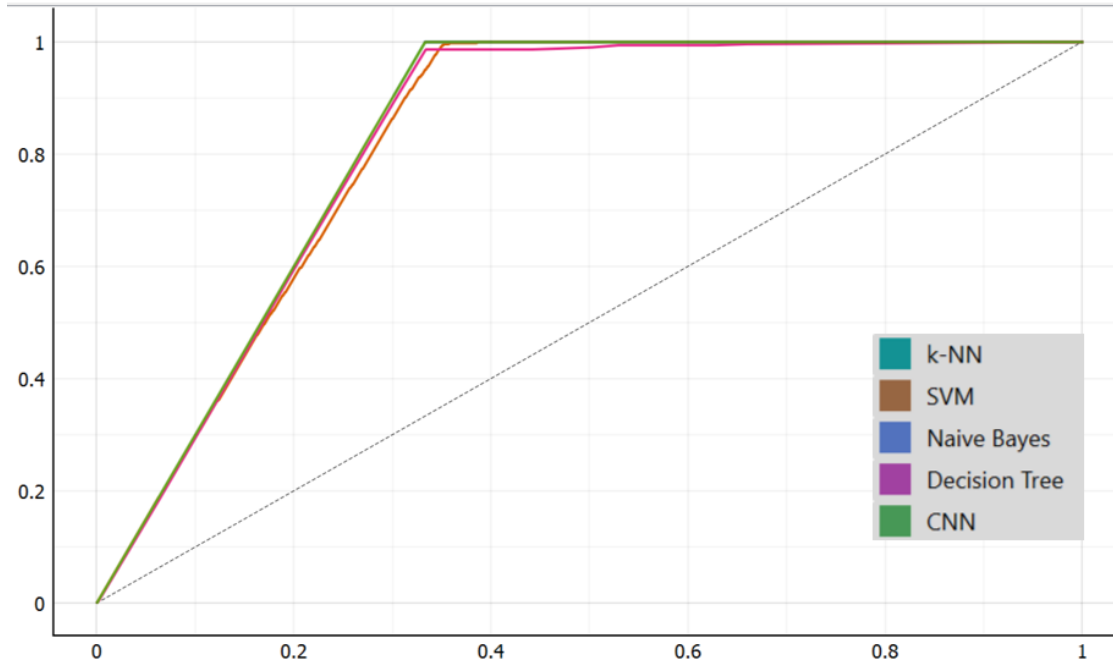


Figure 8: AUC curve of the Palm in anaemia detection

4.1 Comparative Analysis of the Machine Learning Algorithms

For the performance of machine learning models to be evaluated, accuracy, F1-score, AUC, precision, and recall were well-thought-out procedures for evaluating the models. To avoid overfitting of performance for the detection by the models, we utilized a 10-fold cross-validation and validated the models.

The results of the various algorithms for the detection of anemia were considered. The Naïve Bayes achieved the highest accuracy of 98.96% when tested on the palpable palm, although the Convolutional Neural Network (CNN) had an accuracy of 99.12%. The Support Vector Machine (SVM) attained the lowest accuracy of 95.34%. The Naïve Bayes, Decision Tree and k-NN obtained an accuracy of 98.96%, 98.29% and 98.92% respectively when tested on the palpable palm dataset.

There were no significant variations in the performance of the models between the colour of the fingernails and the conjunctiva of the eyes when tested. CNN achieved an accuracy of 98.45% in the conjunctiva and 98.33% in the fingernails. The Decision Tree obtained an accuracy of 97.32%, 97.96%, and 89.45% obtained by the k-NN and the SVM respectively when tested on the

conjunctiva of the eye images. On the other hand, the SVM achieved an accuracy of 92.69% , while the k-NN, Decision Tree, and Naïve Bayes achieved an accuracy of 97.89%, 97.18 and 94.94, respectively, when tested on the colour of the fingernails dataset.

The results obtained from the proposed models used in this study are a clear indication that the palm is an accurate part of the human body to be used to detect iron-deficiency anemia with the Naïve Bayes as its corresponding model in the detection of iron-deficiency anemia. Moreover, the CNN performed better than the Naïve Bayes when the conjunctiva and the colour of the fingernails were trained, validated and tested.

4.2 Conclusion

This paper aimed to detect iron deficiency anemia, comparing machine learning models (CNN, Naïve Bayes, Decision Tree, k-NN and SVM) performance. The models were trained, validated, and tested on images of the conjunctiva of the eyes, palpable palm and colour of the fingernails. The CNN had a higher accuracy than all the models when tested on the fingernails, palpable palm, and conjunctiva images. Furthermore, the performance of the models in the palm had a higher accuracy than that of the fingernails and conjunctiva when tested with the data set.

The results obtained by the models show that the CNN is robust and performs better than Naïve Bayes, Decision Tree, k-NN and SVM in anemia detection and the palpable palm is one of the reliable human features for anemia detection in children due to its higher detection accuracy.

[24] indicated that pallor (palpable) palmer is the best detector of anemia among the conjunctiva, fingernails, and tongue. [31] [6] also stated that the palpable palm gives a significant accuracy in the detection of anemia than the conjunctiva of the eyes, mostly for children under the age of 5 to 59 months, even though the conjunctiva of the eyes is mostly used for the detection of anemia, especially with the use of the non-invasive method.

[24] detected anemia by evaluating the effectiveness of the conjunctiva, tongue, nailbed (fingernails), and the palm on their aetiology relationship. The study showed that the palm had higher accuracy to detect anemia, followed by the conjunctiva and then the fingernails, while the tongue gave the least accuracy. [32] conducted a study on anemia detection using the pallor of the conjunctiva, tongue, nailbed, and palm. The datasets were derived from children (participants) of

6 – 59 months. The results obtained by [32] concluded that the palm achieved the highest sensitivity of 58% to detect anemia which was moderated and when combined with the conjunctiva and palm sensitivity was increased to 73%.

The palm is simple to examine compared to the eyes, which is challenging to access the conjunctiva and the region of interest, particularly for children below 6 years whose eyes may often be exposed to falling. Additionally, minors' eyes would be opened to take pictures or examine the conjunctiva of the eyes directly. There is a chance that someone's finger could get in their eyes [6]. This can be a potential infection source.

The performance (detection accuracy) of the models would have a great impact on the health facilities concerning the detection of iron-deficiency anemia due to the effectiveness and efficient performance of the proposed models. According to the massive performance of the models obtained by this study, the results would have a great impact on health facilities worldwide, especially in health facilities in rural Ghana where access to health facilities, equipment or resources and health professionals is scarce.

Ethics and Consent for this study

The ethics committee of the hospitals enlisted in this study approved the collection of the dataset before the study started. Moreover, since the participants (patients) used for the study were minors, ethical consent was requested from their parent(s) or guardian(s) and the aim and objectives of the study were discussed with them with the benefits it would be the health services. Consent was approved by their parents (parents) or guardians (children) before the participants were enrolled in data collection. Moreover, the Committee for Human Research and Ethics (CHRE) at the University of Energy and Natural Resources, Sunyani approved (Reference number: CHRE/CA/042/22) the commencement of this work. Furthermore, the names and faces of the patients or participants were not shown or exposed during the capture of the images, which makes their identities unknown.

Conflict of Interest.

The authors assert that they do not have a conflict of interest in any form in this study.

Authors' Contributions

PA analysed the data, conception, or design of the work. JWA collected the data and analysed the algorithms. ETD and GD analyzed the data for interpretation and critically analyzed the article. All authors read and approved the article.

Datasets Published on a Repository

The datasets used for this study have been published in a repository as listed below;

1. Asare, Justice Williams; APPIAHENE, PETER; DONKOH, EMMANUEL (2022), “Detection of Anemia using Colour of the Fingernails Image Datasets from Ghana”, Mendeley Data, V1, doi: 10.17632/2xx4j3kjg2.1
2. Asare, Justice Williams; APPIAHENE, PETER; DONKOH, EMMANUEL (2022), “Anemia Detection using Palpable Palm Image Datasets from Ghana”, Mendeley Data, V1, doi: 10.17632/ccr8cm22vz.1
3. APPIAHENE, PETER; ASARE, JUSTICE WILLIAMS; DONKOH, EMMANUEL (2022), “Application of Machine Learning in Detecting Iron Deficiency Anemia Using Conjunctiva Image Dataset from Ghana”, Mendeley Data, V1, doi: 10.17632/nt7r8hv2pz.1

Appendix A: List of Hospitals where Datasets were collected

Hospital	City/Town	Total Dataset
Ahmadiyya Muslim Hospital	Tachiman	128
Bolgatanga Regional Hospital	Bolgatanga	95
Ejusu Government Hospital	Ejusu	41
Holy Family Hospital	Berekum	8
Kintampo Municipal Hospital	Kintampo	60
Komfo Anokye Teaching Hospital	Kumasi	134
Manhyia District Hospital	Kumasi	43
Nkawie-Toase Government Hospital	Nkawie-Toase	86
SDA Hospital	Sunyani	15
Sunyani Municipal Hospital	Sunyani	100
Total		710

Reference

- [1] WHO, “Anemia Treatment, prevalence and data status,” Oct. 12, 2019.
https://www.who.int/health-topics/anaemia#tab=tab_3 (accessed Jul. 16, 2022).
- [2] A. A. Al-alimi, S. Bashanfer, and M. A. Morish, “Prevalence of Iron Deficiency Anemia among University Students in Hodeida Province, Yemen,” *Anemia*, vol. 2018, pp. 1–7, 2018, doi: 10.1155/2018/4157876.
- [3] S.-R. Pasricha, J. Tye-Din, M. U. Muckenthaler, and D. W. Swinkels, “Iron deficiency,” *The Lancet*, vol. 397, no. 10270, pp. 233–248, 2021, doi: 10.1016/s0140-6736(20)32594-0.
- [4] E. O. Tartan, A. Berkol, and Y. Ekici, “Anemia Diagnosis By Using Artificial Neural Networks,” *International Journal of Multidisciplinary Studies and Innovative Technologies*, vol. 4, no. 1, pp. 14–17, 2020.
- [5] M. D. Dithy and V. Krishnapriya, “Anemia selection in pregnant women by using random prediction (Rp) classification algorithm,” *International Journal of Recent Technology and Engineering*, vol. 8, no. 2, pp. 2623–2630, Jul. 2019, doi: 10.35940/ijrte.B3016.078219.
- [6] P. Appiahene, J. W. Asare, E. T. Donkoh, G. Dimauro, and R. Maglietta, “Detection of iron deficiency anemia by medical images: a comparative study of machine learning algorithms,” *BioData Min*, vol. 16, no. 1, p. 2, Jan. 2023, doi: 10.1186/s13040-023-00319-z.
- [7] A. Tamir *et al.*, “Detection of anemia from image of the anterior conjunctiva of the eye by image processing and thresholding,” in *2017 IEEE Region 10 Humanitarian Technology Conference (R10-HTC)*, Dec. 2017, pp. 697–701. doi: 10.1109/R10-HTC.2017.8289053.
- [8] M. Tetschke, P. Lilienthal, T. Pottgiesser, T. Fischer, E. Schalk, and S. Sager, “Mathematical Modeling of RBC Count Dynamics after Blood Loss,” *Processes*, vol. 6, no. 9, p. 157, 2018, doi: 10.3390/pr6090157.
- [9] G. Dimauro, D. Caivano, and F. Girardi, “A New Method and a Non-Invasive Device to Estimate Anemia Based on Digital Images of the Conjunctiva,” *IEEE Access*, vol. 6, pp. 46968–46975, 2018, doi: 10.1109/ACCESS.2018.2867110.

- [10] “Who has the highest risk of developing anemia?” 2019. [Online]. Available: <https://www.ekfdiagnostics.com/who-has-the-highest-risk-of-developing-anemia.html>
- [11] World Health Organization, “Anemia Treatment, prevalence and data status.” Apr. 2019. [Online]. Available: https://www.who.int/health-topics/anaemia#tab=tab_3
- [12] G. Dimauro, A. Guarini, D. Caivano, F. Girardi, C. Pasciolla, and A. Iacobazzi, “Detecting Clinical Signs of Anaemia From Digital Images of the Palpebral Conjunctiva,” *IEEE Access*, vol. 7, pp. 113488–113498, 2019, doi: 10.1109/access.2019.2932274.
- [13] A. Mitani *et al.*, “Detection of anaemia from retinal fundus images via deep learning,” *Nat Biomed Eng*, vol. 4, no. 1, pp. 18–27, Jan. 2020, doi: 10.1038/s41551-019-0487-z.
- [14] T. Mazzu-Nascimento *et al.*, “Smartphone-based photo analysis for the evaluation of anemia, jaundice and COVID-19,” *International Journal of Nutrology*, vol. 14, no. 02, pp. e55–e60, Aug. 2021, doi: 10.1055/s-0041-1734014.
- [15] S. Kasiviswanathan, T. Bai Vijayan, L. Simone, and G. Dimauro, “Semantic Segmentation of Conjunctiva Region for Non-Invasive Anemia Detection Applications,” *Electronics (Basel)*, vol. 9, no. 8, p. 1309, 2020, doi: 10.3390/electronics9081309.
- [16] R. G. Mannino *et al.*, “Smartphone app for non-invasive detection of anemia using only patient-sourced photos,” *Nat Commun*, vol. 9, no. 1, 2018, doi: 10.1038/s41467-018-07262-2.
- [17] G. Kesavaraj and S. Sukumaran, “A study on classification techniques in data mining,” *2013 Fourth International Conference on Computing, Communications and Networking Technologies (ICCCNT)*, 2013, doi: 10.1109/icccnt.2013.6726842.
- [18] T. Karagül Yıldız, N. Yurtay, and B. Öneç, “Classifying anemia types using artificial learning methods,” *Engineering Science and Technology, an International Journal*, vol. 24, no. 1, pp. 50–70, 2021, doi: 10.1016/j.jestch.2020.12.003.
- [19] N. J. Peksi, B. Yuwono, and M. Y. Florestiyanto, “Classification of Anemia with Digital Images of Nails and Palms using the Naive Bayes Method,” *Telematika*, vol. 18, no. 1, p. 118, Mar. 2021, doi: 10.31315/telematika.v18i1.4587.

- [20] Dr. J. Verma and P. Arjun, "Diabetes Mellitus Prediction using Ensemble Machine Learning Techniques," *International Journal of Recent Technology and Engineering (IJRTE)*, vol. 9, no. 2, pp. 312–316, 2020, doi: 10.35940/ijrte.b3480.079220.
- [21] A. Irum, M. Akram, S. M. Ayub, S. Waseem, and M. J. Khan, "Anemia Detection using Image Processing," in *The International Conference On Digital Information Processing, Electronics, And Wireless Communications*, 2016.
- [22] P. M. Wightman Rojas, L. A. Mass Noriega, and A. Salazar Silva, "Hemoglobin screening using cloud based mobile photography applications [Online First]," *Ingenieria y Universidad*, vol. 23, no. 2, Jun. 2019, doi: 10.11144/Javeriana.iyu23-2.hsuc.
- [23] G. Delgado-Rivera *et al.*, "Method for the automatic segmentation of the palpebral conjunctiva using image processing," in *2018 IEEE International Conference on Automation/XXIII Congress of the Chilean Association of Automatic Control (ICA-ACCA)*, 2018, pp. 1–4.
- [24] D. K. K., K. S. Avabratha, K. V. Shenoy, and A. K. V., "Efficacy of site of pallor to detect anemia and its correlation with etiology in under five children," *Int J Contemp Pediatrics*, vol. 8, no. 1, p. 160, Dec. 2020, doi: 10.18203/2349-3291.ijcp20205429.
- [25] P. Jain, S. Bauskar, and M. Gyanchandani, "Neural network based non-invasive method to detect anemia from images of eye conjunctiva," *Int J Imaging Syst Technol*, vol. 30, no. 1, pp. 112–125, 2019, doi: 10.1002/ima.22359.
- [26] N. Djuric, M. Grbovic, and S. Vucetic, "Distributed Confidence-Weighted Classification on Big Data Platforms," 2015, pp. 145–168. doi: 10.1016/B978-0-444-63492-4.00007-1.
- [27] S. Aneja *et al.*, "Deep Neural Network to Predict Local Failure Following Stereotactic Body Radiation Therapy: Integrating Imaging and Clinical Data to Predict Outcomes," *International Journal of Radiation Oncology*Biography*Physics*, vol. 99, no. 2, p. S47, 2017, doi: 10.1016/j.ijrobp.2017.06.120.
- [28] P. T. Dalvi and N. Vernekar, "Anemia detection using ensemble learning techniques and statistical models," in *2016 IEEE International Conference on Recent Trends in Electronics, Information and Communication Technology, RTEICT 2016 - Proceedings*, Jan. 2017, pp. 1747–1751. doi: 10.1109/RTEICT.2016.7808133.

- [29] V. Bevilacqua *et al.*, “A novel approach to evaluate blood parameters using computer vision techniques,” in *2016 IEEE International Symposium on Medical Measurements and Applications (MeMeA)*, May 2016, pp. 1–6. doi: 10.1109/MeMeA.2016.7533760.
- [30] A. Naik and L. Samant, “Correlation review of classification algorithm using data mining tool: WEKA, Rapidminer, Tanagra, Orange and Knime,” *Procedia Comput Sci*, vol. 85, pp. 662–668, 2016.
- [31] S. Chand, F. Shaikh, C. Das, Y. Memon, M. A. Nizamani, and Z. A. Q. Baloch, “Anemia in children with palmar pallor aged 02 months to 05 years,” *Indo American Journal of Pharmaceutical Sciences*, vol. 4, no. 2, 2017.
- [32] T. Getaneh, T. Girma, T. Belachew, and S. Teklemariam, “The utility of pallor detecting anemia in under five years old children.,” *Ethiop Med J*, vol. 38, no. 2, pp. 77–84, 2000.